Spectroscopy of $A\ ^3\Sigma^+ \leftarrow X\ ^1\Sigma^+$ and $B\ ^3\Pi \leftarrow X\ ^1\Sigma^+$ transitions in CdNe and CdAr molecules

R. Bobkowski,* M. Czajkowski, and L. Krause
Department of Physics, University of Windsor, Windsor, Ontario, Canada N9B 3P4
and Ontario Laser and Lightwave Research Centre, Windsor, Ontario, Canada N9B 3P4
(Received 31 August 1989)

Excitation spectra of CdNe and CdAr van der Waals molecules were produced in a molecular beam employing free-jet supersonic expansion, crossed with a pulsed dye-laser beam. Bands arising from $A\ ^3\Sigma^+ \leftarrow X\ ^1\Sigma^+$ and $B\ ^3\Pi \leftarrow X\ ^1\Sigma^+$ transitions between vibrational levels were analyzed, yielding spectroscopic constants for the three states. Computer simulations of the bands combined with the application of the London dispersion relation led to values for r_e, the equilibrium internuclear separations. The effective lifetimes of the CdAr($^3\Sigma^+$) and CdAr($^3\Pi$) molecules in various vibrational states were also determined and were found to be affected by quenching collisions.

I. INTRODUCTION

During the past several decades, there have been numerous investigations of van der Waals molecules,[1,2] though spectroscopic studies of these weakly bound species only became possible with the development of tunable lasers and supersonic jet expansion techniques.[3-7] In recent years, several articles were published dealing with the spectroscopy of metal–noble-gas van der Waals dimers.[3,4,8-10] We report here on the spectra of CdNe and CdAr molecules produced in a jet expansion beam and excited from their $X\ ^1\Sigma^+$ ground states to the lowest excited $A\ ^3\Sigma^+$ and $B\ ^3\Pi$ states. These experiments constitute an extension to previous studies of these dimers[8,9] but they also reveal some new and interesting effects yielding, in addition, the lifetimes of the $A\ ^3\Sigma^+$ and $B\ ^3\Pi$ molecules in specific vibrational states.

II. EXPERIMENTAL PROCEDURE

A detailed description of the apparatus and experimental procedure has been given previously.[11,12] The spectra were excited in an evacuated expansion chamber into which Cd atoms seeded in Ar or Ne as a carrier gas were injected through a nozzle constituting part of the beam source. The latter was made of stainless steel and consisted of an oven and a nozzle, and was heated by a differential heating system. The resulting supersonic beam was crossed (at right angles) with a pulsed laser beam and the optical excitation took place in the region of the intersection.

The oven containing Cd of 99.999% purity (supplied by Metron) was maintained at a temperature of around 700 K and the nozzle at about 770 K, as measured with thermocouples affixed on the oven and the nozzle. The diameter of the nozzle (D) was 150 μm and the distance X between the nozzle and the laser beam varied between 6 and 10 mm, depending on the pressure P_0 of the carrier gas in the oven. The relatively low temperature of the source, at which the spectrum of Cd_2 molecules was suppressed,[11] ensured the purity of the CdAr and CdNe spectra. We used relatively high carrier-gas pressures since the best results were obtained with 8 atm of Ar or 10 atm of Ne; at higher pressures it would have been necessary to work at larger X values at which there are undesirable side effects, as will be explained below. The dye laser employed a 600-line grating at grazing incidence, producing an output linewidth of 0.2 cm^{-1}. Its output wavelength was calibrated against an optogalvanic spectrum[13] and was monitored during the experiments by a Fizeau-wedge wavemeter.[14] The fluorescence emitted perpendicularly to the plane of the crossed beams was passed through a UG5 filter and was detected with an EMR541-N-03-14 photomultiplier whose signal was registered with an EG&G 162/166 boxcar integrator and recorded with an X-Y plotter. The boxcar integrator, the wavemeter, and the laser were connected to the PC-XT computer which stored the data and controlled the scanning of the dye laser.[12]

III. RESULTS AND DISCUSSION

A. The CdNe excitation spectrum

Figure 1 shows a trace of the CdNe excitation spectrum which includes two vibronic bands arising from $A\ ^3\Sigma^+ \leftarrow X\ ^1\Sigma^+$ and $B\ ^3\Pi \leftarrow X\ ^1\Sigma^+$ transitions. The trace contains a few additional vibrational components in the $B \leftarrow X$ band and one additional component in the $A \leftarrow X$ band, which were not seen in the course of earlier observations[8] where the $A \leftarrow X$ band was overlaid by the strong $^3P_1 \leftarrow {}^1S_0$ atomic line. Table I lists the frequencies of the vibrational components in the two bands, representing the averages of five scans carried out under varying conditions of excitation ($40 \le X/D \le 65$, $8 \le P_0 \le 13$ atm). The $B\ ^3\Pi \leftarrow X\ ^1\Sigma^+$ progression includes a "hot band" ($v' = 1 \leftarrow v'' = 1$). Figure 2 shows the Birge-Sponer plot for the vibrational components of the $B \leftarrow X$ band, which yielded the spectroscopic constants for the $B\ ^3\Pi$ state that are listed in Table II. The vibrational frequency ω_e'' and anharmonicity $\omega_e'' x_e''$ for the $X\ ^1\Sigma^+$ state were obtained from the hot band,[8] and the ground-state dissociation energy was calculated using the relation

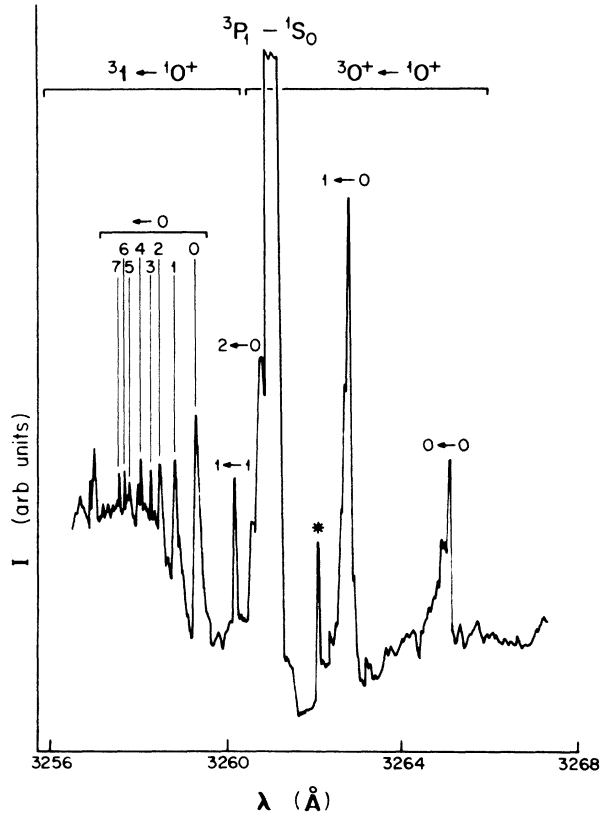

FIG. 1. $A\,{}^30^+ \leftarrow X\,{}^10^+$ and $B\,{}^31 \leftarrow X\,{}^10^+$ excitation spectra of CdNe, showing v' progressions, as well as two hot bands. $T=750$ K, $P_0=10$ atm Ne, $X/D=50$. The trace contains an unidentified band (*).

$$D_e''=T_e'+D_e'-\tilde{\nu}(^3P_1-{}^1S_0)\ . \tag{1}$$

Table II contains all the spectroscopic constants determined in this investigation, as well as those quoted previously.[8] The present results are generally consistent with the earlier values and we ascribe most of the discrepancies to the more accurate wavelength calibration of our dye laser. We can offer no explanation for the difference of 16 cm^{-1} between our $T_e'(A\,{}^30^+)$ value and that quoted in Ref. 9; it is too large to be due to a systematic or statistical error. The table also includes r_e' and r_e'', the equilibrium internuclear separations in the ground and excited states. Kvaran *et al.*[9] determined the rotational constants B_e'' and B_e' for CdNe and hence obtained $r_e''=4.26$ Å and $r_e'(A\,{}^30^+)=3.62$ Å. The value of r_e'' calculated from the London dispersion relation[12,15] agrees remarkably well with this experimental value.

TABLE I. Frequencies of vibronic transitions in CdNe.

	$B\,{}^31 \leftarrow X\,{}^10^+$ band		$A\,{}^30^+ \leftarrow X\,{}^10^+$ band	
$v' \leftarrow v''$	$\tilde{\nu}$ (cm^{-1})	ΔG (cm^{-1})	$\tilde{\nu}$ (cm^{-1})	ΔG (cm^{-1})
0←0	30 670.7		30 621.3	
		4.3		19.7
1←0	30 675.0		30 641.0	
		3.3		17.2
2←0	30 678.3		30 658.2	
		2.5		
3←0	30 680.8			
		2.1		
4←0	30 682.9			
		2.1		
5←0	30 685.0			
		1.0		
6←0	30 686.0			
		0.5		
7←0	30 686.5			
1←1	30 663.2			

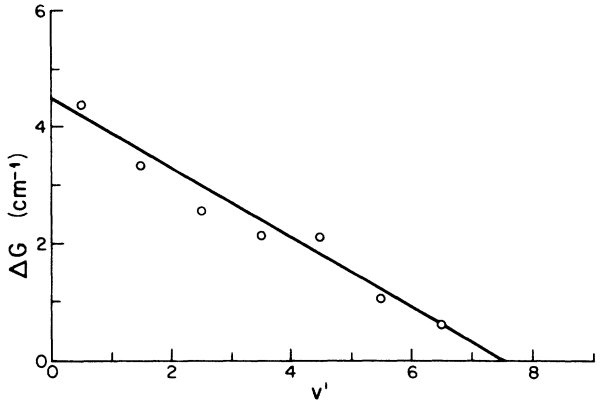

FIG. 2. A Birge-Sponer plot of the v' progression in the $B\,{}^31 \leftarrow X\,{}^10^+$ spectrum of CdNe.

To obtain r_e', we carried out a computer simulation of the spectrum shown in Fig. 1, calculating the Franck-Condon (FC) factors and using the Morse potential as an approximate representation of the ground and excited states. The best fit of the simulated spectrum to the experimental spectrum, shown in Fig. 3, yields $r_e'-r_e''$ and hence r_e', since r_e'' is known. The estimated error in the r_e' values depends on the sensitivity of the computer fit. In the case of the $B\,{}^31$ state the fit is much more sensitive than for the $A\,{}^30^+$ state, and the error is correspondingly smaller. It should also be noted that in the latter case $r_e'-r_e''$ is negative, indicating that $r_e''>r_e'$, as indicated by the shading or degradation of the vibrational components in the $A\,{}^30^+ \leftarrow X\,{}^10^+$ band towards shorter wavelengths. On the other hand, the vibrational components in the $B\,{}^31 \leftarrow X\,{}^10^+$ band are shaded towards longer wavelengths, suggesting that $r_e''<r_e'$, as confirmed by the results of the computer simulation.

The computer modeled $B \leftarrow X$ band shown in Fig. 3 reproduces faithfully the experimental spectrum. The modeling procedure was less successful with the $A \leftarrow X$ band, suggesting that the Morse potential is an adequate representation of the $X\,{}^10^+$ and $B\,{}^31$ states but not of the $A\,{}^30^+$ state. It was found that when the latter state was represented by a variation of the Lennard-Jones potential at large internuclear separations, the correlation between the experimental and computer simulated $A \leftarrow X$ spectra was quite satisfactory.[9,10]

TABLE II. Spectroscopic constants for CdNe.

Designation	$B\,^3\Pi_1(^3\Sigma)$	$A\,^3\Pi_0^+(^3\Pi)$	$X\,^1\Sigma_0^+(^1\Sigma)$
ω_0' (cm^{-1})	4.5[a];5.2[b]	21.3[a];19.5[b]	
ω_0'' (cm^{-1})			12.0[a];13[b]
$\omega_0''x_0''$ (cm^{-1})			1.12[a];1.3[b]
$\omega_0'x_0'$ (cm^{-1})	0.3[a];0.4[b]	1.42[a];1.6[b]	
D_0'' (cm^{-1})			32.0[a];33[b]
D_0' (cm^{-1})	17.0[a];18[b]	80.0:[a];66[b]	
D_e'' (cm^{-1})			38.0[a];39[b]
D_e' (cm^{-1})	19.3[a];21[b]	90.6[a];75[b]	
ω_e'' (cm^{-1})			13.0[a]
ω_e' (cm^{-1})	4.8[a]	22.7[a]	
$\omega_e''x_e''$ (cm^{-1})			1.12[a]
$\omega_e'x_e'$ (cm^{-1})	0.3[a]	1.42[a]	
T_e' (cm^{-1})	30 674.5[a]	30 603.5[a]	
$r_e'-r_e''$ (Å)	0.7±0.03[a]	−1.0±0.05[a]	
r_e'' (Å)			4.1±0.2[c]
			4.26±0.05[d]
r_e' (Å)	4.8±0.2[a,c]	3.10±0.2[c]	
	4.96±0.05[a,e]	3.62±0.05[d]	

[a]This work.
[b]Reference 8.
[c]This work, calculated from the London dispersion relation and D_e''.
[d]Reference 9.
[e]Calculated from Ref. 9.

B. The CdAr excitation spectrum

The excitation spectrum of CdAr was produced at various values of P_0 and X, and various source temperatures, chosen so as to observe the largest possible number of vibrational components. A trace of the spectrum, which contains the $A\,^3\Pi_0^+ \leftarrow X\,^1\Sigma_0^+$ and $B\,^3\Pi_1 \leftarrow X\,^1\Sigma_0^+$ bands, is shown in Fig. 4. The spectrum was obtained with P_0 in the range 6–8 atm and $X=10$ mm, which is equivalent to an effective Mach number $M_{\text{eff}} \simeq 50$ with $D=150$ μm. The temperature of the source was near 680 K at which the Cd_2 spectrum was suppressed. The frequencies of the vibrational components listed in Table III represent average values resulting from five separate scans. The reproducibility of the measurements was very good, which accounts for the small error in the ΔG values shown in Table III. The assignments of the v' components in the $A \leftarrow X$ band coincide with those of Kvaran *et al.*[9] and the assignments in the $B \leftarrow X$ band agree with those of Kowalski, Czajkowski, and Breckenridge.[8] The Birge-Sponer plots of the two bands which are shown in Fig. 5 yielded values of ω_0', $\omega_0'x_0'$, and D_0', assuming that the Morse potential was representative of all three states, which is justified by the linearity of the Birge-Sponer plots. It is also apparent that the $B\,^3\Pi_1 \leftarrow X\,^1\Sigma_0^+$ band includes all the v' levels in the $B\,^3\Pi_1$ state. The vibrational frequency ω_0'' of the ground state was calculated from the two hot bands in the $B \leftarrow X$ spectrum and the bond strength D_0'' was estimated using Eq. (1). The various

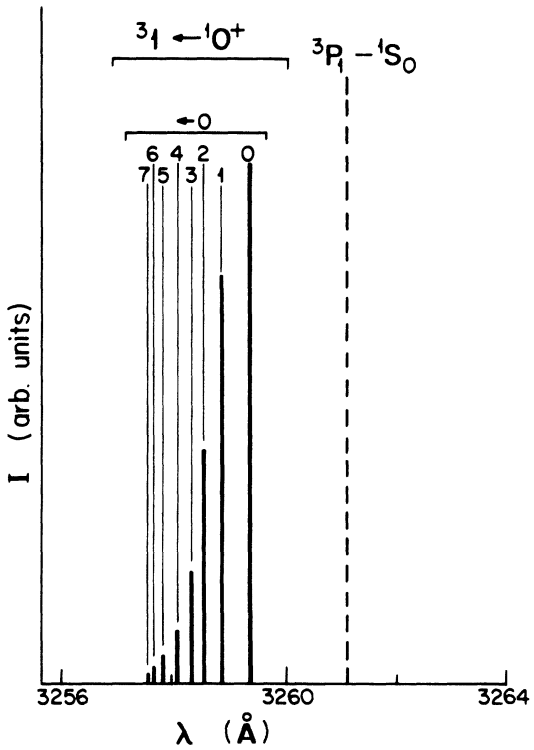

FIG. 3. Computer simulation of the $B\,^3\Pi_1 \leftarrow X\,^1\Sigma_0^+$ excitation spectrum of CdNe showing relative intensities of the vibrational components.

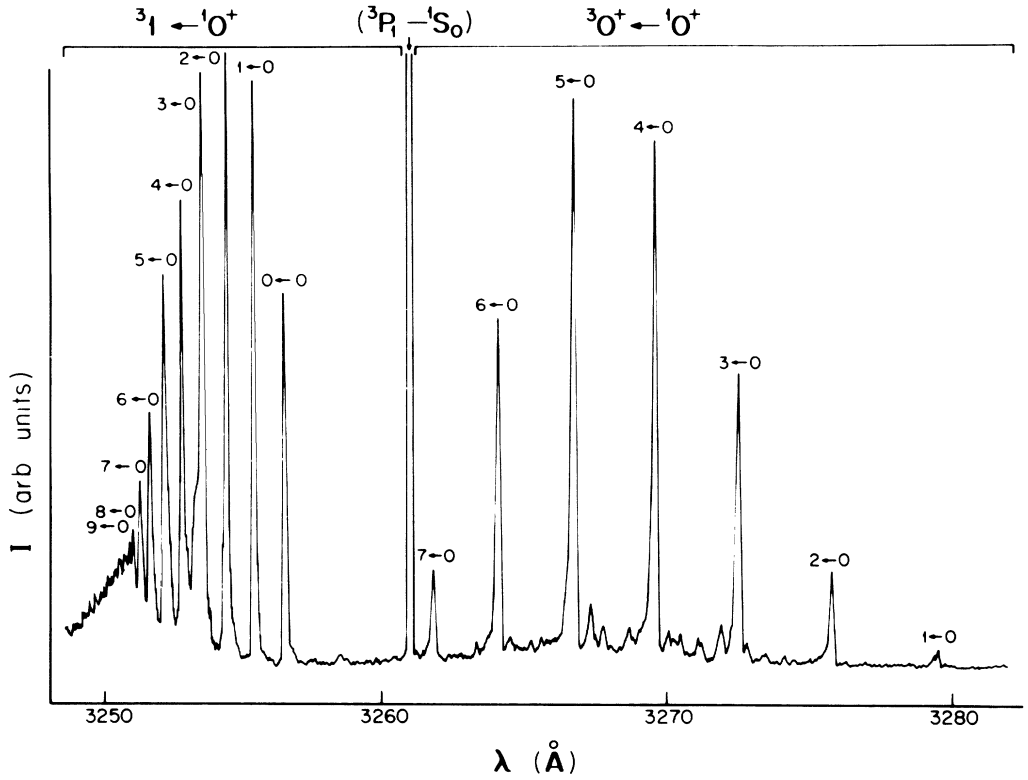

FIG. 4. $A\,^3O^+ \leftarrow X\,^1O^+$ and $B\,^3\Pi \leftarrow X\,^1O^+$ excitation spectra of CdAr showing v' progressions. $T=710$ K, $P_0=6$ atm Ar, $X/D=50$. The region of the $A \leftarrow X$ band contains several unidentified small peaks.

TABLE III. Frequencies of vibronic transitions in CdAr. Asterisk denotes a value obtained from extrapolation.

	$B\,^3\Pi \leftarrow X\,^1O^+$ band		$A\,^3O^+ \leftarrow X\,^1O^+$ band	
$v' \leftarrow v''$	$\tilde{\nu}$ (cm^{-1})	ΔG (cm^{-1})	$\tilde{\nu}$ (cm^{-1})	$\Delta\tilde{\nu}$ (cm^{-1})
0←0	30 707.8		30 449.7*	
		10.6		37.0
1←0	30 718.4		30 486.7	
		9.3		35.3
2←0	30 727.7		30 522.0	
		8.4		31.0
3←0	30 736.1		30 553.0	
		7.0		28.8
4←0	30 743.0		30 581.8	
		5.9		27.0
5←0	30 748.9		30 608.8	
		4.9		25.0
6←0	30 753.8		30 633.8	
		3.5		22.5
7←0	30 757.3		30 656.3	
		2.4		
8←0	30 759.7			
		1.8		
9←0	30 761.5			
		0.4		
10←0	30 761.9			

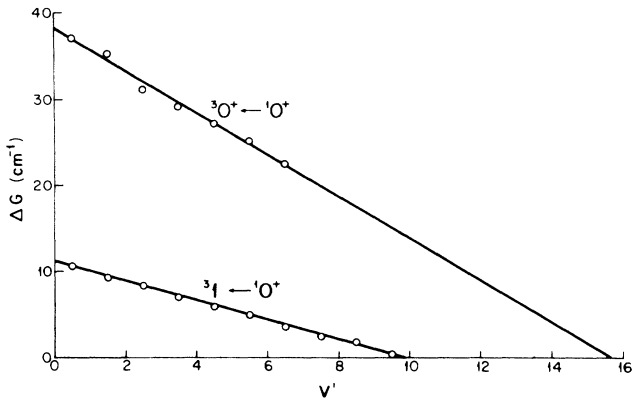

FIG. 5. Birge-Sponer plots of the v' progressions in the $A\,^3\Omega^+ \leftarrow X\,^1\Omega^+$ and $B\,^3\Pi \leftarrow X\,^1\Omega^+$ spectra of CdAr.

spectroscopic constants are compared in Table IV with values reported elsewhere. As before, we ascribe the discrepancies between our results and those reported in Ref. 8 to a more accurate wavelength calibration of our dye laser.

We calculated the equilibrium internuclear separation r_e'' in the ground state using the London dispersion relation[12,15] and using the available ionization potentials[16] and polarizabilities.[17] The resulting value is in excellent agreement with that obtained from the experimentally determined rotational constants B_e''.[9] As in the case of CdNe, we calculated the FC factors for the v' progressions in the $A \leftarrow X$ and $B \leftarrow X$ bands and carried out a computer simulation of the spectra using $r_e' - r_e''$ as the adjustable parameter. The best fit of the $B \leftarrow X$ spectrum, shown in Fig. 6, yielded values of $r_e' - r_e''$ and hence the r_e'

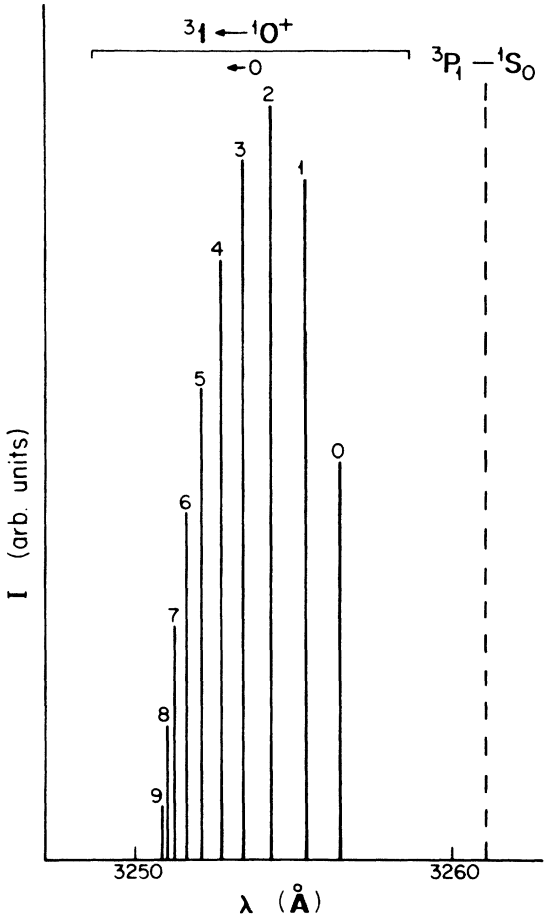

FIG. 6. Computer simulation of the $B\,^3\Pi \leftarrow X\,^1\Omega^+$ excitation spectrum of CdAr, showing relative intensities of the vibrational components.

TABLE IV. Spectroscopic constants for CdAr.

Designation	$B\,^3\Pi(^3\Sigma)$	$A\,^3\Omega^+(^3\Pi)$	$X\,^1\Omega^+(^1\Sigma)$
ω_0' (cm^{-1})	11.1[a];11.1[b]	38.1[a]	
ω_0'' (cm^{-1})			18.9[a];20.0[b]
$\omega_0''x_0''$ (cm^{-1})			0.92[a];1.00[b]
$\omega_0'x_0'$ (cm^{-1})	0.51[a];0.61[b]	1.22[a]	
D_0'' (cm^{-1})			97.0[a];96[b]
D_0' (cm^{-1})	54.0[a];51[b]	303.0[a]	
D_e'' (cm^{-1})			106.5[a];106[b]
D_e' (cm^{-1})	59.7[a];56.0[b]	322[a];325[c];326[d]	
ω_e'' (cm^{-1})			19.82[a]
ω_e' (cm^{-1})	11.7[a]	39.2[a];38.5[a]	
$\omega_e''x_e''$ (cm^{-1})			0.92[a]
$\omega_e'x_e'$ (cm^{-1})	0.57[a]	1.22[a];1.22[c]	
T_e' (cm^{-1})	30 702.5[a]	30 440.4[a];30 437[c]	
$r_e' - r_e''$ (Å)	0.7±0.03 Å[a]	−0.8±0.03 Å[a]	
r_e'' (Å)			4.3±0.3[a];4.33±0.03[c] 3.49[d]
r_e' (Å)	5.03±0.03[a]	3.50±0.03[a];3.45±0.03[c] 3.38[d]	

[a]This work, calculated from the London dispersion relation and D_e''.
[b]Reference 8.
[c]Reference 9.
[d]Reference 18.

values which are also listed in Table IV and are fully consistent with values quoted elsewhere. We found the fit to be very sensitive to changes in $r_e' - r_e''$, which accounts for the small estimated errors quoted in the table though, as before, the fit was better in the case of the $B \leftarrow X$ band than the $A \leftarrow X$ band (not shown) suggesting that the Morse potential is not a satisfactory representation of the $A\ ^3\Omega^+$ state. We note again that in the B state $r_e' > r_e''$ and in the A state $r_e' < r_e''$, as confirmed by the "red shading" and "blue shading," respectively, of the vibrational components.

Using the various molecular constants given in Tables II and IV and the Morse potential, we constructed potential-energy (PE) curves for the $A\ ^3\Omega^+$, $B\ ^3\Pi$, and $X\ ^1\Omega^+$ states of CdNe and CdAr, which are shown in Figs. 7 and 8.

C. The use of the London dispersion relation in simulations of CdN and HgN spectra

In the analysis of the CdNe and CdAr spectra we used the London dispersion relation to represent the interaction energy in the van der Waals molecules and obtained sensible results consistent with experimental measurements. To provide additional justification for the use of this relation,[12] we carried out simulations of additional CdN and HgN (N representing a noble gas) spectra and compared the results with those reported by other authors.

The computer simulations of the $A \leftarrow X$ and $B \leftarrow X$ bands of CdKr which were produced experimentally elsewhere,[8] yielded values of r_e'' ($X\ ^1\Omega^+$) and r_e' for the $A\ ^3\Omega^+$ and $B\ ^3\Pi$ states which are listed in Table V. r_e' ($A\ ^3\Omega^+$) is in reasonable agreement with the calculation of Czuchaj and Sienkiewicz[18] who used Baylis's pseudopotentials.[19] Simulations were also performed on the $A \leftarrow X$ and $B \leftarrow X$ bands of HgN molecules which were observed in recent experiments of Fuke, Saito, and Kaya[3] and Yamanouchi *et al.*[4] Using their experimental data and the Morse potential we simulated the $A \leftarrow X$ and $B \leftarrow X$ bands of HgNe, HgAr, HgKr, and HgXe and obtained values $r_e' - r_e''$. The corresponding ground-state equilibrium internuclear separations r_e'' were estimated using the London dispersion relation together with ionization potentials[16] and polarizabilities,[17] and experimental D_0'' values. As may be seen in Table VI, the results are remarkably close to the values derived from the experiments.[3,4] The computer modeled spectra were also found to be in satisfactory agreement with the experimental traces of both $A \leftarrow X$

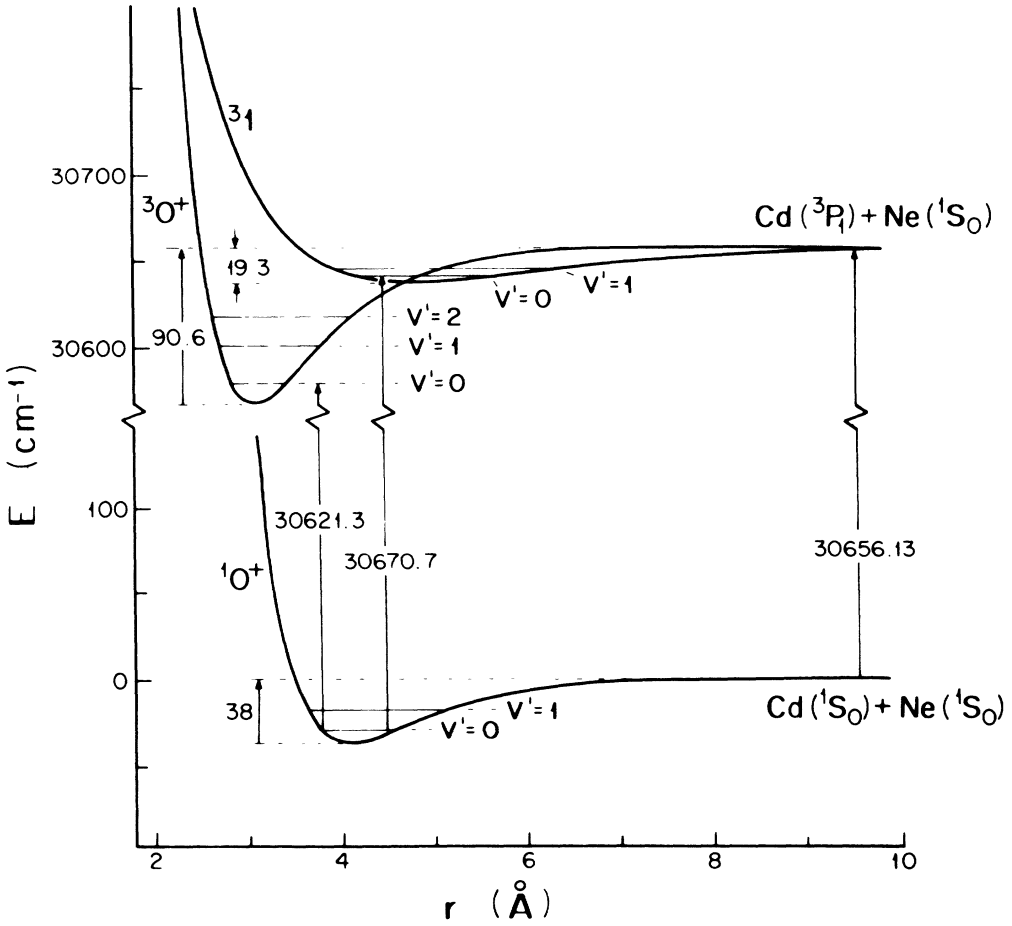

FIG. 7. A PE diagram for CdNe calculated from the experimental data using the Morse potential.

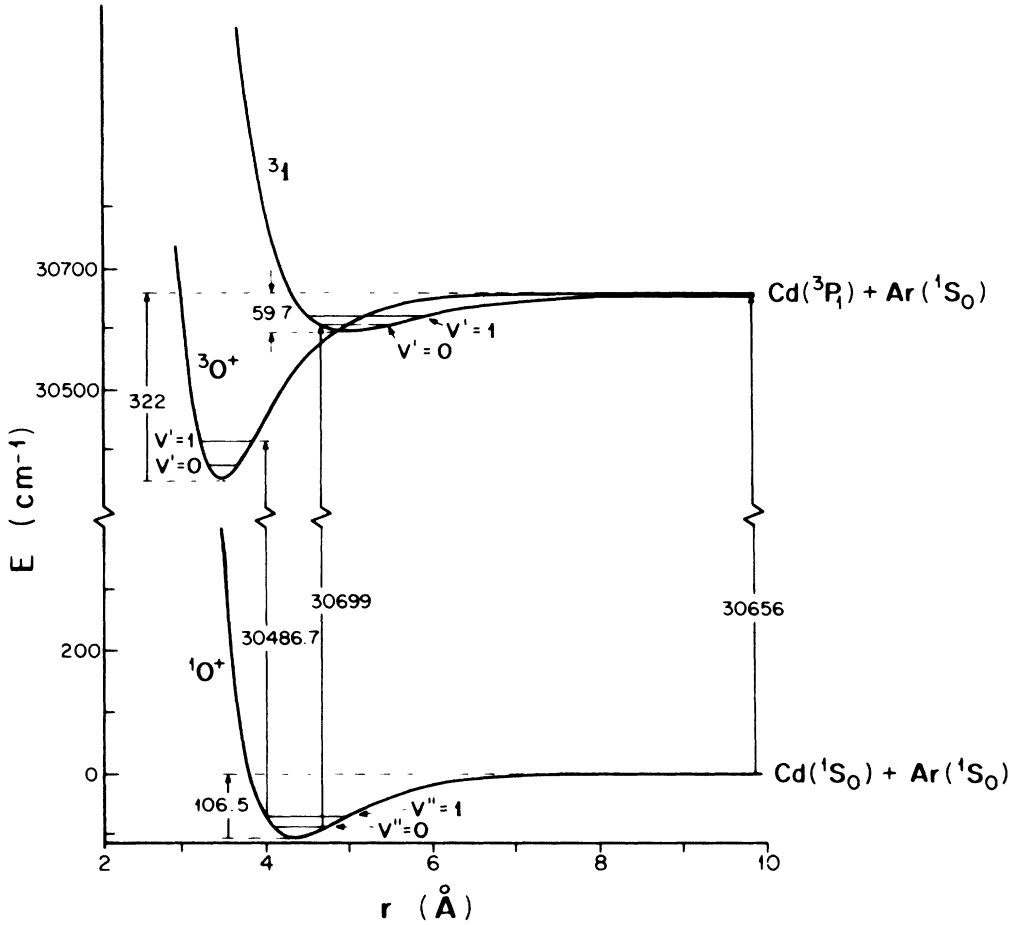

FIG. 8. A PE diagram for CdAr calculated from the experimental data using the Morse potential.

and $B \leftarrow X$ bands in all the HgN molecules. A similar conclusion was reached by Fuke, Saito, and Kaya[3] who, however, constructed their molecular potentials using the Rydberg-Klein-Rees method and their experimental data and effected a satisfactory comparison with the Morse potential.

We believe that the high degree of agreement between the equilibrium internuclear separations calculated using the London dispersion relation and the Morse potential, and those taken from other sources, justifies our use of these devices in the analysis of the CdNe and CdAr spectra.

D. Measurement of the CdAr lifetimes

As the laser was tuned to excite particular v' levels of the $A\,^3\Sigma^+$ or $B\,^3\Pi$ state of CdAr, large fluorescence signals were produced whose persistence times were easily determined, enabling us to determine the effective lifetimes of the various vibrational states. (The corresponding signals from CdNe were much fainter and no measurements of their persistence times were attempted.) The resulting lifetimes are listed in Table VII. It appears that there is some variation in the lifetimes, with the highest vibrational states having the shortest lifetimes. In the case of the $B\,^3\Pi$ state the lifetimes appear to decrease uniformly from $v'=1$ to $v'=7$, which we ascribe to collisions of CdAr with Ar atoms in the beam. Since, in this experiment, we used $P_0=10$ atm, $X=8$ mm, $T=725$ K, and $X/D=54$, the effective Mach number M_{eff} was 48 and the terminal Mach number M_T was 62

TABLE V. Equilibrium internuclear separations in the $B\,^3\Pi$, $A\,^3\Sigma^+$, and $X\,^1\Sigma^+$ states of CdKr (Å).

Designation	$B\,^3\Pi(^3\Sigma)$	$A\,^3\Sigma^+(^3\Pi)$	$X\,^1\Sigma^+(^1\Sigma)$
$r_e'-r_e''$	0.47±0.03[a]	−0.55±0.05[a]	
r_e''			4.40±0.3[c]
r_e'	4.9±0.2[a]	3.85±0.3[a]	
		3.44[b]	

[a]Obtained from computer simulation.
[b]Reference 18.
[c]Calculated from the London dispersion relation and D_e''.

TABLE VI. Equilibrium internuclear separations in the $B\,^3\mathrm{1}$, $A\,^3\mathrm{0}^+$, and $X\,^1\mathrm{0}^+$ states of HgNe, HgAr, HgKr, and HgXe (Å).

Designation	$B\,^3\mathrm{1}(^3\Sigma)$	$A\,^3\mathrm{0}^+(^3\Pi)$	$X\,^1\mathrm{0}^+(^1\Sigma)$
		HgNe	
$r_e'-r_e''$	0.85±0.03[a]	−1.2±0.1[a]	
r_e''			3.87[b];3.87[c]
r_e'	4.72[b];4.57[c]	2.67[b];3.12[c] 3.44[b]	
		HgAr	
$r_e'-r_e''$	0.6±0.03[a]	−0.65±0.1[a]	
r_e''			4.05[b];4.01[c]
r_e'	4.65[b];4.66[c]	3.4[b];3.38[c]	
		HgKr	
$r_e'-r_e''$	0.51±0.01[a]	−0.62±0.1[a]	
r_e''			4.15[b];4.07[c]
r_e'	4.66[b];4.57[c]	3.53[c];3.52[c]	
		HgXe	
$r_e'-r_e''$	0.22±0.01[a]	−1.2±0.3[a]	
r_e''			4.20[b];4.25[d]
r_e'	4.42[b];4.47[d]	3.0±0.3[b];3.25[d]	

[a]Obtained from the best fit of Franck-Condon factors calculated from the Morse potential to the experimental results of Ref. 3.
[b]Calculated for the ground state using the London dispersion relation and D_e'' from Ref. 3, or for the excited states using $(r_e'-r_e'')$ values from the best fit as in footnote a.
[c]From Ref. 3.
[d]From Ref. 4.

and, consequently, the particles in the beam must have been subjected to collisions.[7] This conclusion was confirmed by the value of the Cd $5\,^3P_1$ atomic lifetime which was measured simultaneously and was found to be 2.4 μs, whereas the radiative lifetime is 3.0 μs.[11] To produce a collisionless beam, it would have been necessary to make $M_{\text{eff}} \geq M_T$, but this requires $X_{\min} \simeq 13$ mm, a distance from the nozzle at which the density of beam and the fluorescence intensity are greatly decreased.

We believe that in low vibrational states the molecular lifetime tends to be rather longer and close to the atomic lifetime, since some activation energy is required to cause a quenching transition by way of the atomic energy state. If the collision frequency is higher than the transition probability, at higher vibrational levels less energetic collisions can dissociate the molecules, thus depressing the effective lifetime. That this trend appears to be much more pronounced in the $B\,^3\mathrm{1}$ state than in the $A\,^3\mathrm{0}^+$ state, may be due to the relative shift of the $A\,^3\mathrm{0}^+$ and $X\,^1\mathrm{0}^+$ PE curves seen in Fig. 8 and to the accompanying differences in the transition probabilities.[20]

TABLE VII. Effective lifetimes of various $B\,^3\mathrm{1}$ and $A\,^3\mathrm{0}^+$ vibrational states in CdAr.

	$\tau(\mu\text{s})$	
v' state	$B\,^3\mathrm{1}$	$A\,^3\mathrm{0}^+$
0	2.3±0.1	
1	2.7±0.1	
2	2.7±0.1	2.3±0.1
3	2.6±0.1	2.4±0.1
4	2.5±0.1	2.6±0.1
5	2.4±0.1	2.7±0.1
6	2.2±0.1	2.3±0.1
7	2.0±0.1	2.0±0.1

IV. SUMMARY AND CONCLUSIONS

$A\,^3\mathrm{0}^+ \leftarrow X\,^1\mathrm{0}^+$ and $B\,^3\mathrm{1} \leftarrow X\,^1\mathrm{0}^+$ excitation spectra of CdNe and CdAr were produced in a supersonic expansion beam crossed with a laser beam. Analyses of the vibrational structures, combined with computer simulation of the spectra based on the Morse potential and with a simple application of the London dispersion relation, yielded molecular constants, including equilibrium internuclear separations for the three states, summarized in Tables II and IV. The applicability of these methods was

verified by comparison with results reported elsewhere for other CdN and HgN van der Waals molecules. PE curves for CdNe and CdAr, constructed on the basis of the data obtained in this investigation, are shown in Figs. 7 and 8. The lifetimes of individual vibrational states in CdAr were measured and were found affected by collisional quenching.

ACKNOWLEDGMENTS

This research was supported in part by the Natural Sciences and Engineering Research Council of Canada. One of us (R.B.) was partially supported under Project No. CPBP01.06 from the Institute of Physics, Nicholas Copernicus University, Toruń, Poland.

---

*On leave from the Institute of Physics, Nicholas Copernicus University, Toruń, Poland.

[1]J. C. Miller and L. Andrews, J. Chem. Phys. **69**, 3034 (1978).

[2]J. C. Miller and L. Andrews, Appl. Spectrosc. Rev. **16**, 1 (1980), and references within.

[3]K. Fuke, T. Saito, and K. Kaya, J. Chem. Phys. **81**, 2591 (1984).

[4]K. Yamanouchi, J. Fukuyama, H. Horiguchi, S. Tsuchiya, K. Fuke, T. Saito, and K. Kaya, J. Chem. Phys. **85**, 1808 (1986).

[5]R. Campargue, J. Chem. Phys. **52**, 1795 (1970).

[6]R. Campargue, Rev. Sci. Instrum. **35**, 111 (1964).

[7]D. M. Lubman, C. T. Rettner, and R. N. Zare, J. Chem. Phys. **86**, 1129 (1982).

[8]A. Kowalski, M. Czajkowski, and W. Breckenridge, Chem. Phys. Lett. **121**, 217 (1985).

[9]A. Kvaran, D. J. Funk, A. Kowalski, and W. H. Breckenridge, J. Chem. Phys. **89**, 6069 (1988).

[10]D. J. Funk, A. Kvaran, and W. H. Breckenridge, J. Chem. Phys. **90**, 2915 (1989).

[11]M. Czajkowski, R. Bobkowski, and L. Krause, Phys. Rev. A **40**, 4338 (1989).

[12]M. Czajkowski, R. Bobkowski, and L. Krause, Phys. Rev. A **41**, 277 (1990).

[13]J. R. Nestor, Appl. Opt. **21**, 4554 (1982).

[14]W. Kedzierski, J. B. Atkinson, and L. Krause, Opt. Lett. **14**, 607 (1989).

[15]F. London, Z. Phys. **63**, 243 (1930); Z. Phys. Chem. Abt. B **11**, 222 (1930).

[16]C. E. Moore, *Atomic Energy Levels,* Natl. Bur. Stand. Ref. Data Ser., Natl. Bur. Stand. (U.S.) Circ. No. 35 (U.S. GPO, Washington, D.C., 1971), Vols. 1–3.

[17]T. M. Miller and B. Bederson, *Advances in Atomic and Molecular Physics,* edited by D. R. Bates and B. Bederson (Academic, New York, 1977), Vol. 13.

[18]E. Czuchaj and J. Sienkiewicz, J. Phys. B **17**, 2251 (1984).

[19]W. E. Baylis, J. Chem. Phys. **51**, 2665 (1969).

[20]G. Herzberg, *Spectra of Diatomic Molecules* (Van Nostrand, New York, 1950).